Multiquanta Vortex Entry and Vortex-Antivortex Pattern Expansion in a Superconducting Microsquare with a Magnetic Dot

Carlos Carballeira,[1,*] Victor V. Moshchalkov,[1] Liviu F. Chibotaru,[2] and Arnout Ceulemans[2]

[1]*Nanoscale Superconductivity and Magnetism Group, INPAC–Institute for Nanoscale Physics and Chemistry, K.U. Leuven, Celestijnenlaan 200 D, 3001 Leuven, Belgium*

[2]*Quantum Chemistry Group, INPAC–Institute for Nanoscale Physics and Chemistry, K.U. Leuven, Celestijnenlaan 200 F, 3001 Leuven, Belgium*

(Received 6 July 2005; published 2 December 2005)

We investigate the nucleation of superconductivity in a microsquare with a magnetic dot on top. The cusplike behavior of the calculated normal-superconducting phase boundaries, $T_c(H)$, shows a transition between short-period to long-period oscillations when going from positive to negative applied fields, H. Vorticity changes by more than 1, indicating multiquanta vortex entries, have been detected along this asymmetric $T_c(H)$ boundary. The dot also expands dramatically the symmetry-consistent vortex-antivortex patterns, thus facilitating their experimental observation.

DOI: 10.1103/PhysRevLett.95.237003 PACS numbers: 74.78.Na, 74.20.De, 74.25.Dw, 75.75.+a

The intrinsic quantum nature of superconductivity makes superconductors with dimensions of the order of $\xi(0)$, the Ginzburg-Landau (GL) coherence length, particularly sensitive to confinement effects. In the past years, significant advances in different nanofabrication techniques have promoted the systematic study of the properties of micro- and nanosuperconductors [1]. This research has demonstrated that the topology of the sample can be used to enhance considerably the superconducting critical parameters, thus opening new perspectives for the potential applications of superconductivity. Moreover, nanostructuring also strongly affects the vortex matter in these superconductors. For instance, in cylindrical geometries, the superconductivity nucleates in the form of a giant vortex in the center [2], while symmetry-consistent vortex-antivortex patterns may be spontaneously created in both triangles [3] and squares [4]. This interest in the confinement effects has been recently extended to hybrid superconductor/ferromagnetic (SF) nanosystems [5,6]. In the case of individual nanostructures, these studies have been focused on a cylindrical symmetry of the superconductor, but they have already revealed new physical phenomena arising from the interaction between superconductivity and magnetism at this submicrometer scale. A good example is the profound influence that a magnetic dot may have on the onset of superconductivity and vortex states in loops and disks [5,6].

In this Letter, we investigate the nucleation of superconductivity in a square with a cylindrical magnetic dot on top. The existing analytic procedure to solve the linearized Ginzburg-Landau equation (LGLE) in regular polygons [7] has been adapted to include the contribution of the dot to the total magnetic field, allowing us to identify new quantum effects in the onset of superconductivity arising from the interplay between the finite rotational symmetry of the square and the inhomogeneous field of the dot. These effects, which include vorticity changes by more than 1 associated with multiquanta vortex entries in the sample and an expansion of the symmetry-consistent vortex-antivortex patterns, are well beyond those expected for a cylindrical geometry of the superconductor [5,6,8].

The most adequate tool to study the nucleation of superconductivity is the LGLE given by [9]

$$\left(-i\nabla - \frac{2\pi}{\phi_0}\mathbf{A}\right)^2 \psi = \frac{1}{\xi^2(T)}\psi. \tag{1}$$

Equation (1) is analogous to the Schrödinger equation [10]. So, as the latter, it will preserve in the solutions the symmetry imposed by the boundary conditions, which in the case of a superconductor-vacuum interface can be written as [9]

$$\left(-i\nabla - \frac{2\pi}{\phi_0}\mathbf{A}\right)\psi|_n = 0. \tag{2}$$

In Eqs. (1) and (2), $\mathbf{A}$ is the vector potential, ϕ_0 is the magnetic flux quantum, ψ is the complex superconducting order parameter, n holds for the normal component to the sample's boundary, and $\xi(T) = \xi(0)(1 - T/T_c)^{-1/2}$.

To overcome the difficulties in solving the LGLE arising from the explicit presence of $\mathbf{A}$ in Eq. (2), it has been proposed to apply a vector potential gauge transformation for regular polygons that, in the case of a homogeneous external field, gives $A_n = 0$ at the sample's boundary [3,4,7]. Equation (2) is then transformed into $\nabla\psi|_n = 0$, and the LGLE may be solved by using an analytic basis set, with corresponding solutions classified according to the irreducible representations (irreps) of the symmetry group of the problem. In a square, with C_4 rotational symmetry, these irreps are denoted as A, B, $E+$, and $E-$, and they correspond to solutions with, respectively, no vortex (vorticity 0), a giant vortex (vorticity $+2$), a vortex (vorticity $+1$), and an antivortex (vorticity -1) in the center of the sample that will be surrounded by a number of vortices

(multiple of 4) that depends on the applied magnetic field H [4]. The calculated vortex patterns are stable close to the phase boundary, but, deeper in the superconducting state, the nonlinear term in the GL equation becomes important and causes symmetry breaking transitions [11].

To study the nucleation of superconductivity in a square with a magnetic dot on top, we have applied the procedure described above to the vector potential resulting from the contributions of the homogeneous external field and the stray field of the dot, this last obtained from magnetostatic calculations. Assuming that the dot is magnetized parallel to the z direction, in cylindrical coordinates such a vector potential reads as [12]

$$A_\varphi = \frac{Hr}{2} + 4M_{\mathrm{dot}}\sqrt{\frac{R}{r}}\int_0^l dz_d \frac{[(1-\frac{k^2}{2})K(k) - E(k)]}{k}, \quad (3)$$

where $A_r = A_z = 0$ and $k^2 = 4Rr/[(R+r)^2 + (z-z_d)^2]$ is a dimensionless variable, the z dependence of which can be used to account for the presence of a substrate between the dot and the sample to avoid proximity effects. Also in the above equation, R, M_{dot}, and l stand for, respectively, the radius, magnetization, and height of the dot, while K and E are, respectively, elliptic integrals of the first and the second kind. Figure 1 shows, together with a schematic drawing of the superconducting square with the magnetic dot on top, the field profile that was obtained from Eq. (3) by using $M_{\mathrm{dot}} = 18\phi_0$, $R = 0.4a$, $l = 0.033a$, and $z = -0.0025a$ (here a is the square's length), parameters that are comparable with those of dots previously used in experiments [6,8]. The details of the gauge transformation of Eq. (3) can be found in Ref. [13].

The magnetic field dependence of the energy of the lowest Landau level corresponding to each irrep in presence of the magnetic dot defined in Fig. 1 is given in Fig. 2(a), together with the results for the no-dot case [Fig. 2(b)]. In order to obtain sample-independent curves, the solutions of Eq. (1) have been multiplied by the sample's surface S, and the magnetic field is presented in units of ϕ/ϕ_0, where $\phi = HS$ is the magnetic flux in the sample. These lowest Landau levels of each irrep define the phase boundaries shown in the insets which, in the no-dot case, are clearly symmetric with respect to the origin [4,13]. This behavior arises from a well-defined sequence of crossings between irreps, A (black line) $\rightarrow E+$ (green line) $\rightarrow B$ (red line) $\rightarrow E-$ (blue line) $\rightarrow A\ldots$, each of them leading to an increase of the total vorticity of the sample, L (that defines the total flux trapped in the square through $L\phi_0$), by 1 [4,13]. However, Fig. 2(a) clearly illustrates that the dot strongly affects this oscillating behavior of the phase boundary. For instance, the $S/\xi^2(T)$ curves are asymmetric with respect to the polarity of the field, giving rise to a maximum critical temperature at, approximately, $\phi \simeq -12.5\phi_0$. This fact clearly indicates the presence of the compensation effect between the stray field of the dot and the applied magnetic field already observed in loops and disks [6], which, as shown by Fig. 2(a), in the square also manifests itself in a long-period oscillation regime between $-38.7 \lesssim \phi/\phi_0 \lesssim -7.8$. Instead, for positive fields the short-period oscillations characteristic of the no-dot case are progressively recovered.

The magnetic dot may also energetically favor one or more irreps with respect to the others, thus leading to changes in the total vorticity of the sample by more than

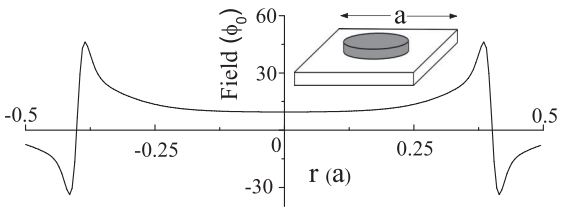

FIG. 1. Calculated field profile of a magnetic dot with $M_{\mathrm{dot}} = 18\phi_0$, $R = 0.4a$, $l = 0.033a$, and $z = -0.0025a$ (here a is the sample's length), together with a schematic drawing of the superconducting square with the magnetic dot on top.

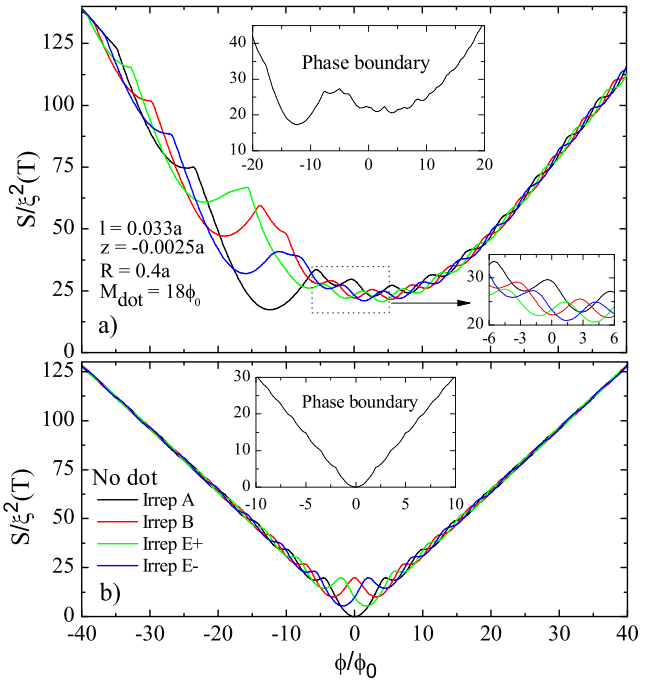

FIG. 2 (color online). (a) Magnetic field dependence of the energy of the lowest Landau level corresponding to each irrep in presence of the magnetic dot presented in Fig. 1, together with (b) the results with no dot. The intersections between these Landau levels determine the phase boundaries shown in the insets. Note the dramatic change in the cusplike behavior of these $S/\xi^2(T)$ curves, from long-period oscillations between $-38.7 \lesssim \phi/\phi_0 \lesssim -7.8$ to short-period oscillations for positive fields. The zoom in (a) illustrates the presence in the phase boundary of transitions between vortex patterns where the vorticity changes by more than 1. X- and Y-axis labels in the insets are the same as in the main figures.

1 (multiquanta transitions) due to the disappearance of transitions between irreps present in the no-dot case. This is already illustrated by the zoom of the $S/\xi^2(T)$ curves shown in Fig. 2(a). In this region bounded by $-6 \lesssim \phi/\phi_0 \lesssim 6$, irreps $E+$ and $E-$ are energetically favored with respect to irreps A and B, and, as a consequence, changes in L by $+2$ associated with the simultaneous entry of two vortices in the sample can be observed at $\phi \simeq -5.1\phi_0$, $\phi \simeq -4\phi_0$, and $\phi \simeq 2.6\phi_0$. However, the presence of multiquanta transitions in the onset of superconductivity can be better observed in Fig. 3, where we present the evolution of the total vorticity of the sample along the phase boundary for four different magnetizations of the dot, namely, $M_{\mathrm{dot}} = 0$ (no dot), $M_{\mathrm{dot}} = 6\phi_0$, $M_{\mathrm{dot}} = 12\phi_0$, and $M_{\mathrm{dot}} = 18\phi_0$. In the no-dot case, $|L|$ shows an almost linear behavior, changing by 1 through field intervals that progressively tend to ϕ_0 when ϕ increases [4]. However, this field dependence dramatically changes when M_{dot} increases. First, as a consequence of the compensation between the external field and the stray field of the dot, the ϕ values at which $|L| = 0$ is observed are shifted to negative fields. In addition, also for negative fields, the vorticity exhibits an oscillating behavior with changes in L by more than 1, which indicates the simultaneous entrance of several vortices into the sample. For instance, at $M_{\mathrm{dot}} = 18\phi_0$ (triangles) and apart from those multiquanta transitions already shown in Fig. 2(a), it is now possible to observe variations in the vorticity by $+4$ from -4 to 0 (along irrep A) and from -14 to -10 (along irrep B), by $+5$ from -10 to -5 (with a change between irreps B an $E-$), and by $+8$ from -27 to -19 (along irrep $E+$). Note that this last big jump in the vorticity appears, approximately, at the same field values at which $S/\xi^2(T)$ curves in Fig. 2(a) enter the long-period oscillations regime.

To illustrate that the origin of the effects on the flux quantization in the square observed in Fig. 3 is the compensation of the applied magnetic field by the stray field of the dot, in Fig. 4 we present the change in the spatial distribution of the squared amplitude of the order parameter ($|\psi|^2$) at the vorticity transitions observed for $\phi = -38.7\phi_0$ [Figs. 4(a) and 4(b)] and $\phi = -7.8\phi_0$ [Figs. 4(c) and 4(d)], the magnetic fields that limit the long-period oscillations regime in Fig. 2(a). As can be seen, the vorticity transition by $+8$ that occurs at $\phi = -38.7\phi_0$ almost coincides (within an interval of, approximately, $0.5\phi_0$) with a profound change in the topology of the order parameter distribution in the square, with the highest values of $|\psi|^2$ (red regions) concentrated in the corners for $\phi < -38.7\phi_0$ (analogously to the no-dot case) but with a ringlike structure when $\phi > -38.7\phi_0$. This $|\psi|^2$ distribution, clearly related to a compensation of the external field by the stray field of the dot, is preserved when the field increases up to $\phi = -7.8\phi_0$. Then $|\psi|^2$ is again higher in the corners, and the well-defined sequence of transitions between irreps is progressively recovered [see Fig. 2(a)]. We have also detected that most of the multiquanta transitions observed in Fig. 3 between $-38.7 \lesssim \phi/\phi_0 \lesssim -7.8$ have the common feature of involving the simultaneous penetration of one or more antivortices (we take as a reference for the vortex-antivortex definition the magnetic moment of the dot) in each of the corners of the square, where there is no field compensation. These results illustrate the importance of the interplay between the finite rotational symmetry of the square and the inhomogeneous field of the dot, which may allow topological changes in

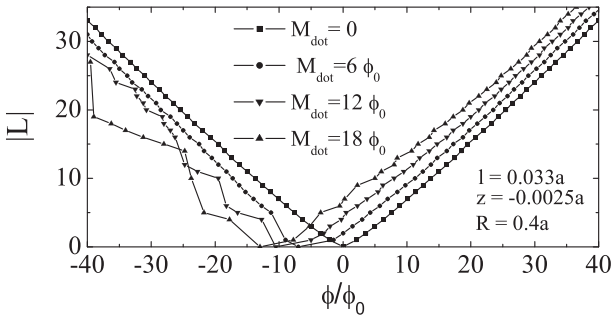

FIG. 3. Magnetic field dependence of the total vorticity of the sample at the normal-superconducting phase boundary for four different magnetizations of the dot. When M_{dot} increases, $|L|$ shows an oscillating behavior for negative ϕ values with vorticity changes by more than 1.

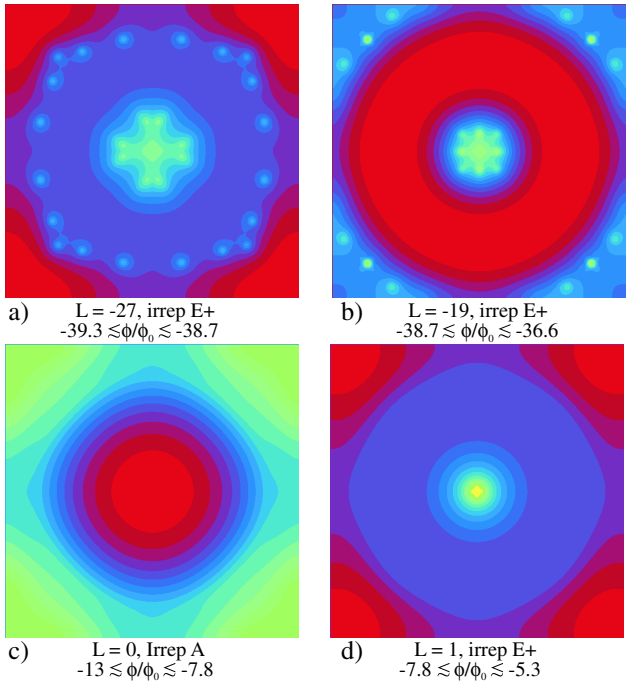

FIG. 4 (color online). Change in the $|\psi|^2$ distribution at the vorticity transitions observed for $\phi = -38.7\phi_0$ [(a) and (b)] and $\phi = -7.8\phi_0$ [(c) and (d)], the magnetic fields that limit the long-period oscillations regime in Fig. 2(a). These transitions coincide with a change in the topology of the vortex patterns that may favor the simultaneous nucleation of one or more antivortices in each one of the corners of the sample.

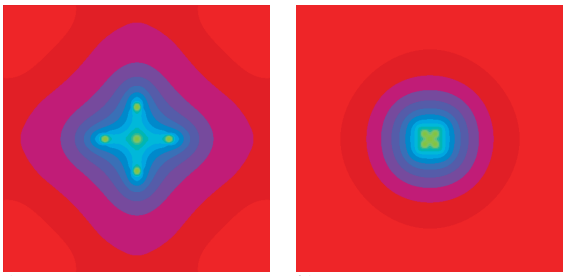

FIG. 5 (color online). A comparison between the vortex-antivortex patterns that can be observed for $L = 3$ (a) with and (b) without the magnetic dot. As can be seen, the vortex pattern rotates 45° and expands dramatically in the presence of the magnetic dot.

the $|\psi|^2$ distribution favoring the nucleation of more than one single vortex along the phase boundary. Similar results have been found for a smaller radius of the dot by using larger values of M_{dot}.

Figure 4 also illustrates that the spontaneous formation of symmetry-consistent vortex-antivortex pairs at the phase boundary in regular polygons is preserved in the presence of a magnetic dot, since the vortex patterns in 4(a) and 4(b) are formed by one vortex in the center surrounded by 28 and 20 antivortices, respectively. In addition, when compared with the $|\psi|^2$ distributions previously obtained in the no-dot case [3,4], Figs. 4(a) and 4(b) also clearly demonstrate that the dot can be used to enlarge these vortex-antivortex patterns, thus facilitating their experimental observation with local vortex-imaging techniques. To further illustrate these results, in Fig. 5 we present a comparison between the order parameter distributions obtained for $L = 3$ with 5(a) and without 5(b) the magnetic dot. Both vortex patterns are formed by an antivortex surrounded by four vortices that, as may be seen, rotate 45° and expand dramatically in the presence of the magnetic dot. This effect can be attributed to the singular behavior of the stray field at the edges of the dot, with both positive and negative large peaks (see Fig. 1) that seem to attract vortices and antivortices.

In conclusion, the interplay between superconductivity and ferromagnetism at submicron scales can give rise to novel quantum effects in the onset of superconductivity of mesoscopic regular polygons with magnetic dots. These effects include multiquanta transitions between vortex patterns and the formation of larger vortex-antivortex patterns than in the no-dot case. From the point of view of the applications, these results open new possibilities to manipulate the flux quantization in superconductor microstructures. Other fundamental aspects of the confinement effects on the superconducting condensate in these hybrid SF nanostructures, such as size and temperature dependence of their properties, deserve further analysis.

This work has been supported by the Research Fund K.U. Leuven GOA/2004/02, the Belgian Interuniversity Attraction Poles, and the Fund for Scientific Research Flanders (FWO). C. C. acknowledges financial support from Fudación Ramón Areces (Spain) through postdoctoral grants and from the Ministerio de Educación y Ciencia (Spain) through MAT2004-04364.

*On leave from LBTS, Departamento de Física da Materia Condensada, Universidade de Santiago de Compostela, E-15782 Santiago de Compostela.
Electronic address: fmcharly@usc.es

[1] For a review, see, e.g., V. V. Moshchalkov *et al.*, in *Handbook of Nanostructured Materials and Nanotechnology*, edited by H. S. Naiwa (Academic, San Diego, 1999), Vol. 3, Chap. 9, p. 451. See also V. V. Moshchalkov *et al.*, Nature (London) **373**, 319 (1995).
[2] V. V. Moshchalkov, X. G. Qiu, and V. Bruyndoncx, J. Low Temp. Phys. **105**, 515 (1996); V. A. Schweigert, F. M. Peeters, and P. S. Deo, Phys. Rev. Lett. **81**, 2783 (1998).
[3] L. F. Chibotaru *et al.*, Phys. Rev. Lett. **86**, 1323 (2001); V. R. Misko *et al.*, *ibid.* **90**, 147003 (2003).
[4] L. F. Chibotaru *et al.*, Nature (London) **408**, 833 (2000); J. Bonca and V. V. Kabanov, Phys. Rev. B **65**, 012509 (2002).
[5] For reviews on SF systems, see, e.g., I. F. Lyuksyutov and V. L. Pokrovsky, Adv. Phys. **54**, 67 (2005); A. I. Buzdin, Rev. Mod. Phys. **77**, 935 (2005).
[6] D. S. Golubovic *et al.*, Appl. Phys. Lett. **83**, 1593 (2003); Phys. Rev. B **68**, 172503 (2003); Europhys. Lett. **65**, 546 (2004); M. V. Milosevic, S. V. Yampolskii, and F. M. Peeters, Phys. Rev. B **66**, 024515 (2002).
[7] L. F. Chibotaru *et al.*, Eur. Phys. J. B **27**, 341 (2002).
[8] D. S. Golubovic *et al.*, Phys. Rev. B **71**, 180502(R) (2005).
[9] See, e.g., M. Tinkham, *Introduction to Superconductivity* (McGraw-Hill, New York, 1996), Chap. 4.
[10] See, e.g., L. D. Landau and E. M. Lifshitz, *Quantum Mechanics* (Pergamon, Oxford, 1975), 2nd ed.
[11] L. F. Chibotaru *et al.*, Phys. Rev. B **70**, 094505 (2004).
[12] L. D. Landau and E. M. Lifshitz, *Electrodynamics of Continuum Media* (Pergamon, Oxford, 1984), 2nd ed.
[13] L. F. Chibotaru *et al.*, J. Math. Phys. (N.Y.) **46**, 095108 (2005).